Wetting and deformation of arrays of elastic fibers

Camille Duprat*, Suzie Protiere** & Howard A. Stone *
*Department of Mechanical and Aerospace Engineering, Princeton University, Princeton, NJ 08544
**CNRS, UMR 7190, Institut Jean le Rond d'Alembert, F-75005 Paris, France

Summary We consider a liquid drop deposited on a pair of flexible fibers and show that flexibility, fiber geometry and drop volume are necessary to understand our observations. We identify the conditions for a drop to remain compact with minimal spreading or to cause a pair of elastic fibers to coalesce. In addition, we present quantitative rules in appropriate dimensionless variables to organize all of our observations. We illustrate these ideas with examples for feathers, beetle tarsi, sprays and microfabricated systems.

INTRODUCTION

The wetting of fibrous media has been well-studied because of many environmental and industrial applications,. Most research focuses on drops on single rigid fibers or on the response of large arrays of fibers. However, the elasticity of the fibers is important in most applications, e.g. the matting of feather barbules [1], the shrinkage of porous fiber membranes [2], strengthening of paper upon drying [3], the clumping of the setae of the beetles tarsi upon release of tarsal oil [4], or the collapse of micro or nano pillars array [5]. To better understand these problems we studied the interaction of a mist of drops with a deformable, or flexible, array of fibers (Fig. 1).

Rigid versus flexible fibers

We investigate the behavior of a perfectly wetting drop deposited onto two horizontal flexible fibers, which are clamped at one end at a distance $d_0>\sqrt{2}r$, and are free to deflect at the other end (Fig.1). For a perfectly wetting droplet deposited on two parallel *rigid* fibers, the minimization of surface energy yields three distinct drop shapes depending on the ratio of the distance between the fibers $2d_0$ and their diameter 2r (Fig. 1a). As d_0/r is decreased, the drop evolves from a bridge to a barrel shape, then spreads into a liquid column [6]: drops for $d_0/r > \sqrt{2}$, columns for $d_0/r < 0.57$, and there is non-uniqueness of the shape for $0.57 < d_0/r < \sqrt{2}$.

Flexibility introduces novel features for the dynamics and equilibrium configurations. Below, 2d denotes the distance between the fibers at the drop location. When the drop is placed on the fibers close to the clamped ends, the fibers deflect inward, and the drop moves spontaneously toward the free ends (Fig. 1c, which shows top and side views). As the drop advances, the deflection increases, i.e. d/r continuously decreases. The drop accelerates and elongates then spreads spontaneously between the fibers, which draws them together to finally form a liquid column between coalesced fibers.

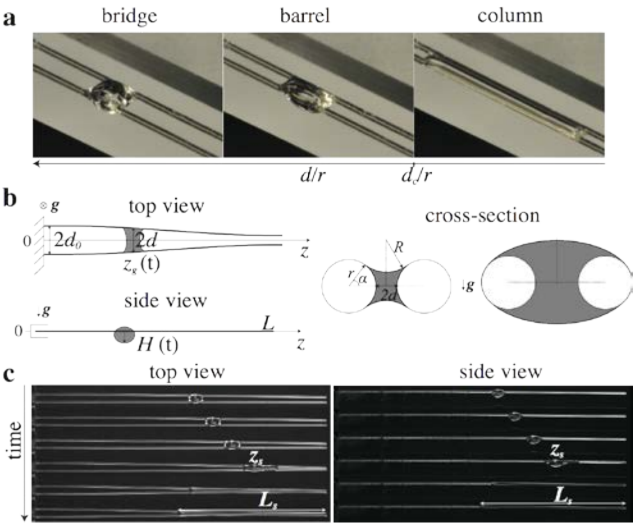

Fig. 1: Shape transitions of a drop sitting on two parallel fibers. a) Drop of perfectly wetting liquid (silicone oil), of volume 2 μL deposited on two parallel rigid glass fibers (radius r = 0.145 mm) adopts three different shapes depending on the distance between the fibers, from a "bridge" ($d_0/r = 2.5$) to a "barrel" ($d_0/r = 1.5$) to a liquid column ($d_0/r = 1$). b) Sketch of the experimental setup used to investigate the behaviour of a drop deposited on two flexible fibers, clamped at one end and free to deflect at the other. Expected cross-section for a concave liquid column or a convex drop. c) Typical experiment with $d_0/r=2.7$, V=1.5μL, L=4 cm. Both top and side views are recorded using a mirror. Time between successive images = 25s. When the drop is deposited on flexible fibers, the fibers deflect inward. The drop spontaneously moves toward the free ends of the fibers. At a given location z_s, the drop starts spreading while the fibers are drawn together. The final wet length is noted L_s.

A UNIVERSAL MAP OF THE FINAL EQUILIBRIA

We performed a large set of experiments to characterize the final state of the drop-on-fiber configuration as a function of the drop volume V, the fiber length L and the ratio d_0/r. For every d_0/r, we find three different final states as L and V are varied (Fig. 2a-c). Whereas the final state (drop or column) of a finite volume of liquid deposited on two rigid fibers only depends on one parameter, i.e. d_0/r, as indicated above, hence is independent of the drop volume and fiber length, we find that the final equilibrium state for a drop on two flexible fibers depends on six parameters, i.e. r, d_0, L, the bending stiffness B of the fiber, the surface tension γ, and the drop volume V. We thus expect that the final states can be determined using three dimensionless parameters. In particular, for short fibers and practically any drop volume, the fibers deflect slightly inward and the drop moves toward the free ends, but there is no spreading (Fig. 2a; in the experimental system shown in Fig. 2 "short" means L<<2cm). For longer fibers, there is a range of drop volumes such that when we increase the length of the fibers L, the deflection increases and the drop spreads completely into a column ("total spreading", Fig. 2c). Alternatively, for sufficiently large volumes, we observe a state of 'partial spreading', where there is a liquid column with a smaller drop remaining at the edge (Fig. 2b).

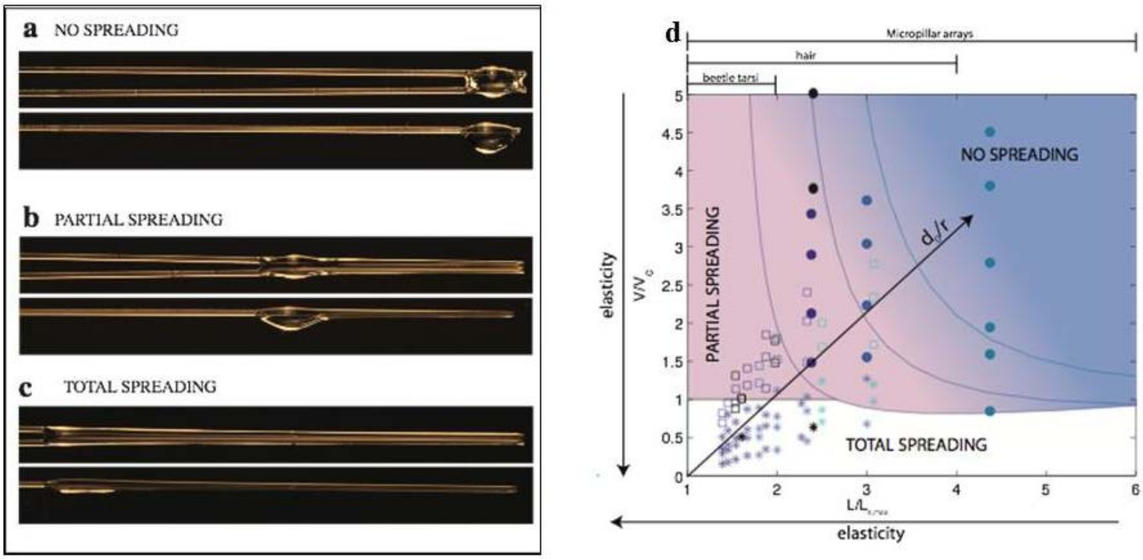

Fig. 2: Three different final states of a drop between two flexible fibers. (a-c): Top and side views obtained for $d_0/r = 2.6$, a fixed volume $V = 2$ μL and increasing length L = 3, 3.5 and 4 cm, transitioning from no spreading to partial spreading to total spreading. a) The drop moves toward the ends without spreading, or b) spreads until partial depletion of the drop, or c) spreads completely into a liquid column. d) Map of the three regimes as a function of the two dimensionless parameters $L/L_{s,max}$ and V/V_c. Three limits for increasing d_0/r ($d_0/r=2.4$, $d_0/r=2.7$, $d_0/r=4.2$) and data points for total spreading (✳), partial spreading (❑) and no spreading (●). Blue-purple points: silicone oil (total wetting) and black-grey points: water (partial wetting) and $d_0/r = 2.1$ and 3 respectively.

We can rationalize our results by analyzing the elastocapillary force and torque balances that characterize the equilibrium states. For example, we can understand the maximum spreading length $L_{s,max}$ reached at a critical volume V_c as a balance between elasticity and capillarity. By minimizing the total energy of the system [7], we identify a maximum value L_{dry} along which the dry portions of the fibres can be bent by capillary forces,

$$L_{dry} = \left(\frac{9Bd_0^2}{2\gamma r S(\alpha)} \right)^{1/4}$$

where $S(\alpha)$ is a geometric factor, evaluated approximately for a flat liquid column as $S(\alpha = \pi/2) = \pi-2$. L_{dry} is the minimum length of the fibers above which collapse can occur. For a given d_0/r, L_{dry} is constant and the maximum wet length $L_{s,max}$ increases linearly with fiber length L, i.e. $L_{s,max} = L-L_{dry}$, which is in good agreement with our experiments. This elastocapillary balance results in a critical volume $V_c = A(\alpha)L_{s,max}$, for which the spreading length is maximal, and where $A(\alpha)$ is the column cross-section ($A(\pi/2) \approx \pi r^2$ for a flat column). In addition, with d_s the spacing where spreading starts to occur, a further calculation that is more involved identifies a critical volume for spreading

$$V_s \approx \Gamma \left(\frac{\gamma d_s r L^3}{B(d_0 - d_s)} \right)^3 ,$$

where the constant Γ only depends on the complex shape of the drop; this result involves all the geometric and material properties. The boundaries for spreading/coalescence $V=V_s$ and total/partial spreading $V=V_c$ are in good agreement with the experiments (Fig. 2d). Finally, we identify the three relevant dimensionless parameters as d_0/r, $L/L_{s,max}$ and V/V_c (Fig. 2d).

CONCLUSIONS

We have provided a detailed study of elastocapillary effects for a droplet wetting a pair of flexible fibers. The six different physical parameters needed to characterize the system yield three dimensionless parameters from which we can organize all of our experimental data. Further, quantitative physical arguments yields results for the different transitions we observe.

References

[1] O'Hara, P.D., Morandin, L.A. Effects of sheens associated with offshore oil and gas development on the feather microstructure of pelagic seabirds. *Marine Pollution Bulletin* **60**: 672-678, 2010.
[2] Kamo, J., Hiram, T., Kamada, K. Solvent-induced morphological change of microporous hollow fiber membranes. *J. Membrane Science* **70**: 217-224, 1992.
[3] Hubbe, M.A. Bonding between cellulosic fibers in the absence and presence of dry-strength agents - a review. *BioResources* **1**: 281-318, 2006.
[4] Eisner, T., Aneshansley, D.J. Defense by foot adhesion in a beetle (Hemisphaerota cyanea). *PNAS* **97:** 6568-6573, 2000.
[5] Pokroy, B., Kang, S.H., Mahadevan, L., Aizenberg, J. Self-organization of a mesoscale bristle into ordered, hierarchical helical assemblies. *Science* **323**: 237-240, 2009.
[6] Princen, H. Capillary phenomena in assemblies of parallel cylinders III. Liquid columns between horizontal parallel cylinders. *Journal of Colloid and Interface Science* **34**: 171-184, 1970.
[7] Py, C., Bastien, R., Bico, J., Roman, B. & Boudaoud, a. 3D aggregation of wet fibers. *Europhysics Letters* **77**, 44005 (2007).